Master's Degree Numerical Methods in Engineering

UNIVERSITAT POLITÈCNICA DE CATALUNYA
BARCELONATECH

Computational Mechanics Tools

Simulation Project: Thermo-activated pile foundation

Authors:
Alessio Renan
Mariano Tomás Fernandez
Aren Khaloian

Professors:
Irene Arias
Amir Abdollahi
Natividad Pastor

January 17^{th}, 2020
Academic Year 2019-2020

Contents

Abstract

The Ground Source Heat Pump (GSHP) technology is a clean and efficient way of obtaining energy from the ground to minimize the electrical consumption in a building. The technology takes advantage from the fact that under a certain depth, soil temperature remains more or less constant throughout the whole year. The idea of this simulation is to represent the conditions of the pile to develop a design of it, taking into consideration building loads, lateral soil pressures, self weight and thermal loads generated by the flow of water. The pile is modelled with a slice of pile at 20.0 m depth using a static-general step and quadrilateral, quadratic and axisymmetric stress elements, with that the stresses of the whole model is represented. The model was done using *ABAQUS*, a finite element method software, to represent correctly the loads, stresses and interactions between thermal and mechanical behaviours. To analyse the resistance of the pile, different temperature conditions were modelled to assess the thermal-mechanical stress condition. The results shown that the pile is correctly designed for water temperatures of about 50°C, and the water can be heated up to about 90°C before causing structural damages to the concrete pile.
Moreover, the convergence of the model was checked using mesh refinement and interpolation order (both h and p refinement). Finally, a different boundary condition was adopted to represent the settlement of the pile due to non-infinite stiffness of the soil.

1 Introduction

In certain structures Ground Source Heat Pump (GSHP) technology is used to reduce the consumption of energy for climate purposes by taking advantage of the fact that at certain depth (of about 10.0 m) the soil's temperature remains constant, see Figure 1a. The system consists in creating boreholes where tubes are buried and water flows through it from the surface to a certain depth of the soil. In this way, whether cold water in winter or hot water in summer flows through the pipes in the borehole to its end and the temperature of it stabilize with the temperature at its surroundings as a result of thermal conductivity between water and the soil. A typical configuration for the GSHP system is presented in Figure 1b.
Generally, given the costs of making a borehole in the ground, this borehole is also used to install a structural pile which besides hosting the GSHP installation (inner tube in blue in the Figure 2) also withstands the structural loads.
The installation of about 2500 *energy piles* in the UK from 2005 to 2009 generated savings of about 3500 annual tons of CO_2 emissions, Nicholson et al. 2013 (1).

2 Problem solution

In this chapter, the pile modelled is presented, the description of the model, materials and assumptions made are also outlined before presenting the results. Afterwards, the obtained results are shown considering thermal and structural loads applied.

2.1 Model general description

The model is represented using a slice of 1.0 m using a finite element method software and taking advantage of its symmetry, an axisymmetric model is used to represent the 3D problem into a 2D which is a much more efficient way to solve the problem using the conditions represented in Figure 3a, in this case the plane scheme Ω is the plane to be modelled. In Figure 3b the model analysed with *ABAQUS* is presented, in which the dotted yellow line represents the axisymmetric axis, and the vertical black line on the blue rectangular represents the division between steel pipe and the concrete pile. Reducing the problem size to a 2D

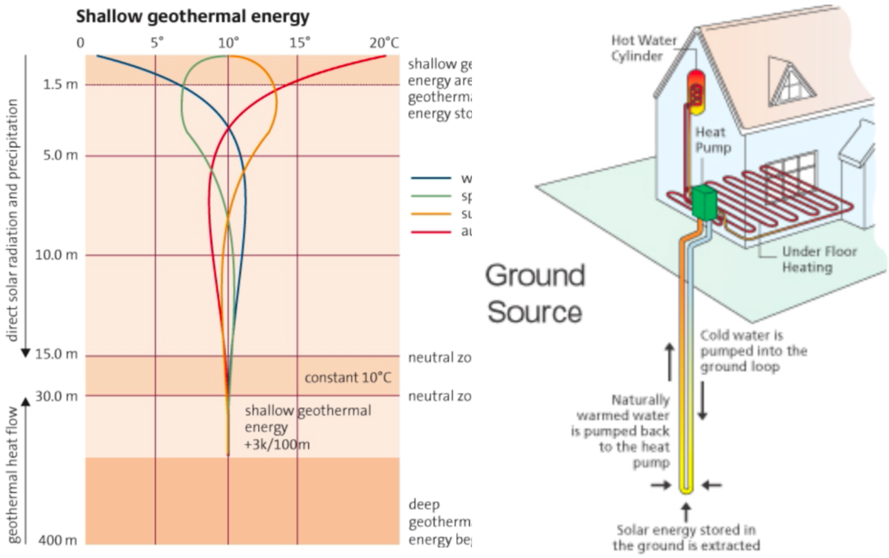

(a) Temperature variation in soil depth

(b) Typical GSHP installation

Figure 1: System presentation.

model, by using axisymmetry model, changes in loads and boundary conditions needs to be adopted, and they are discussed in the following paragraphs.

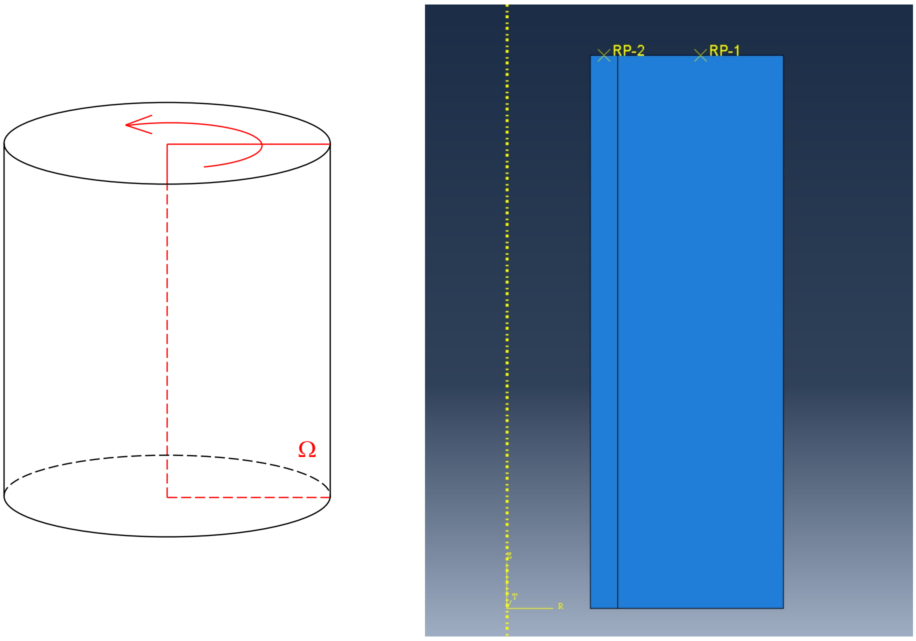

(a) Axisymmetry modelling

(b) FEM model of the pile

Figure 3: Pile model.

2.1.1 Materials

The materials used to model the steel pipe and concrete pile are both linear elastic with characteristics described in Table 1.

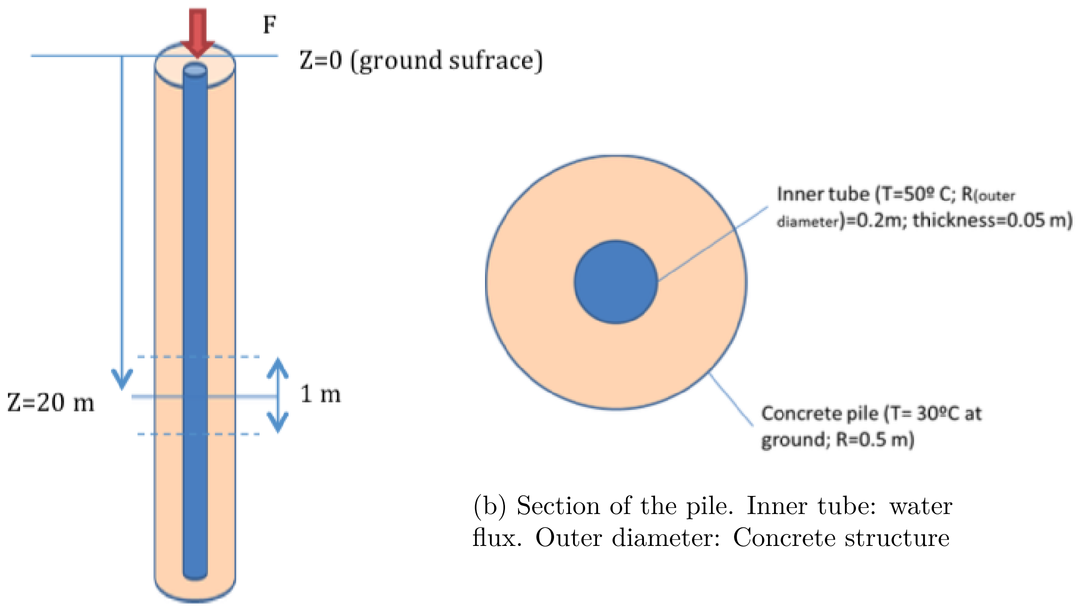

(a) Thermal-structural pile

(b) Section of the pile. Inner tube: water flux. Outer diameter: Concrete structure

Figure 2: Pile geometry.

Material	Young's modulus	Density	Poisson's ratio	Thermal expansion coefficient	Thermal conductivity	Friction angle
-	E [Pa]	[kg/m^3]	-	α [1/°C]	k [W/m·K]	ϕ [°]
Concrete	$2.7 \cdot 10^{10}$	2500	0.2	$1.2 \cdot 10^{-5}$	2	-
Steel	$2.1 \cdot 10^{11}$	7800	0.3	$1.0 \cdot 10^{-5}$	50	-
Soil	-	2000	-	-	-	30

Table 1: Properties of the modelled materials.

2.1.2 Material Contact

The steel tube and the concrete pile have interaction in one layer. The contact between the steel and the concrete layers is prescribed as a normal behaviour-hard contact because of the expansion of the steel in the x direction and a tangential behaviour with friction and penalty factor.The friction coefficient of 0.57 (2) was used between the steel and the concrete. The tangential behaviour was prescribed because the steel tube had expansion in the y direction and the concrete had contraction in the same direction so this will result in tangential contact between the two layers.

2.1.3 Loads

To analyse the problem the following loads were considered:

- Structural loads: A total load of 300 kN due to structural use of the pile was included in the model. In order to include a vertical load in the axisymmetric model and because the force was applied to a refrence point in the middle coupled with the upper surface of the concrete, its value was divided by the length of an arc passing by the mid-point of the concrete pile. In our case, the pile has an outer radius of 0.50 m and an inner diameter of 0.20 m, which results in a mid radius of 0.35 m. Therefore the length of the arc is $\pi \cdot 0.7m = 2.1991m$ and the load to consider in the model is 136.5 kN/m.

- Pile self-weight: Concrete pile self-weight is considered in the model. Its calculation is $\gamma_H \cdot A_p \cdot d_{sup} = 80.4kN$ where $A_p = \pi \cdot (D_{out}^2 - D_{in}^2)/4 = 0.66m^2$ and $D_sup = 19.5m$. Therefore, the load applied must also be corrected by the axisymmetric factor giving us a load of 36.56 kN/m.
- Pipe self-weight: Steel pipe self-weight is considered in the model. Its calculation is $\gamma_S \cdot A_s \cdot d_{sup} = 19.0kN$ where $A_s = \pi \cdot (D_{out}^2 - D_{in}^2)/4 = 0.056m^2$ and $D_{sup} = 19.5m$. Therefore, the load applied must also be applied similarly to the case of the other forces, so it must be divided by the arc of the mid point of the steel which has an outer diameter of 0.20 m, an inner diameter of 0.15 m, so $\pi \cdot 0.35m = 1.098m$ giving us a load of 19.0 kN/m.
- Upper lateral earth pressure: Using equation (1) the lateral pressure coefficient is calculated and replacing $d_i = 19.5m$ in equation (2), the upper lateral pressure is $1.95 \cdot 10^5\ Pa$. Pushing from the external surface of the pile towards the axis of symmetry.
- Lower lateral earth pressure: Calculated replacing $d_i = 20.5m$ in equation (2), the lower lateral pressure is $2.05 \cdot 10^5\ Pa$. Pushing from the external surface of the pile towards the axis of symmetry.
- Upper hydrostatic pressure: Calculated using the upper depth $d_i = 19.5m$ and the specific weight of water $\gamma_w = 10kN/m^3$, the pressure is $1.95 \cdot 10^5\ Pa$. Pushing from the axis of symmetry towards the external surface of the pile.
- Lower hydrostatic pressure: Calculated using the upper depth $d_i = 20.5m$ and the specific weight of water $\gamma_w = 10kN/m^3$, the pressure is $2.05 \cdot 10^5\ Pa$. Pushing from the axis of symmetry towards the external surface of the pile.

$$K_h = 1 - sin(\phi) = 0.5 \tag{1}$$

$$p_i = K_h \cdot \gamma_s \cdot d_i \tag{2}$$

where γ_s is soil's density and d_i are the depths of interest for the upper and lower part of the pile being modelled.

2.1.4 Boundary conditions

To state the boundary conditions of the problem, it is of keen importance to state that the pile modelled has restrictions over the 'r' or 'x' axis. By this, we mean that an horizontal load applied to the surface of the pile, even though there is no restriction in this direction will have to push the whole cylinder and not only the portion seen in Figure 3b. The boundary conditions for the problem are shown in schematic Figure 4a and in Figure 4b the representation on *ABAQUS* is shown. These conditions includes the following aspects:

- Zero vertical displacement on the bottom surface;
- Lateral water loads in the inner surface (in contact with the steel pipe, on the left);
- Lateral earth loads in the outer surface (in contact with the concrete pile, on the right);

- Vertical loads considering both structural and self weight on the top of the concrete pile;
- Vertical loads considering self weight on the top of the steel pipe.

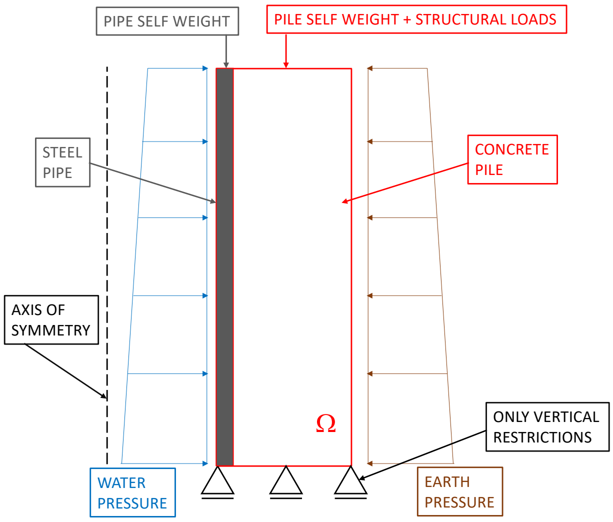

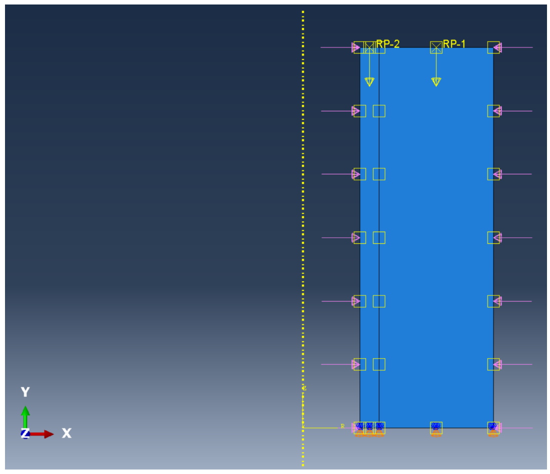

(b) FEM model boundary conditions

(a) Boundary conditions on the FEM model

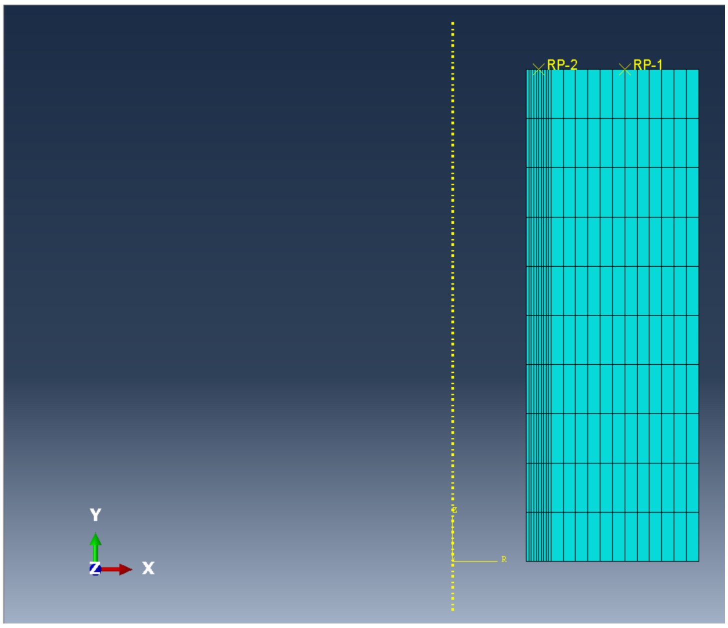

(c) Mesh of the FEM model

Figure 4: Model presentation, mesh and boundary conditions.

2.2 Assignment tasks resolution

2.2.1 Pile stress state subjected to mechanical loads

Analyze the stress state of the concrete and steel pipe of a slice of 1 meter (centered at a depth of 20 m) due to the ground pressure (surface at $z = 0$), as shown in Fig. 2, and a vertical load (F) applied at the top of the pile due to the structure loads of 300 KN (applied only to the concrete section). Consider also the weight of the pile above the section of analysis. The material properties are given in Table 1.
Hint: For the lateral earth pressure, consider the Rankine at rest ($K0 = 1 \;\; \sin\phi$) -no displacement of the pile relative to the soil-. Orient the axis of revolution in the z direction during the assembly of the part instance to enable hydrostatic pressure.

The problem was analysed using the the mesh shown in Figure 4c and from boundary conditions it is mentioned that water is not present, so we don't consider the temperature change and also the hydro static pressure of the water acting on the wall. Obtained results are shown in Figure 5 and it is seen that stresses due to mechanical loads are below 2.0 MPa in the whole pile. We can see that the applied load on the concrete causes some deformation in the concrete and the steel because the contact transfers this stresses to the steel and combined with the self-weight of the steel we can see that the maximum stresses are in the steel. Also because of the higher Young's modulus of steel the stresses created in the steel are higher than the concrete.

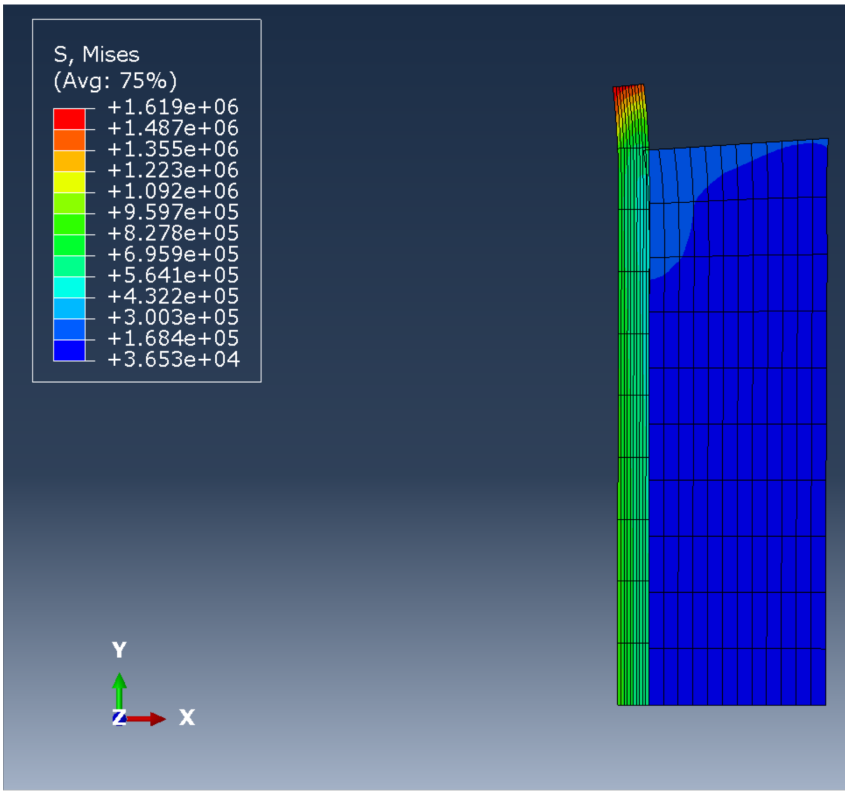

Figure 5: Von Misses stress distribution over the pile. Mechanical loads considered.

2.2.2 Pile stress state subjected to thermal and mechanical loads

Analyze the increase of stresses in the concrete due to the flow of water at 50° C inside the pipe (20° C higher than the ground temperature at z = 20 m, see Figure 2b).
Hint: You may need to reconsider the type of element used for the model to make it appropriate for the type of step calculation.

The problem was analysed using the the mesh shown in Figure 4c and boundary conditions presented in Figure 4a. Temperature effects and the hydro static pressure of the water are considered. Water flows at a temperature of 50°C and the soil surrounding the pile, at a depth of calculus (20.0 m) is at 30°C, therefore the temperature variation from the core of the pipe to the soil is of 20°C. To model this case, we first apply a 30 degrees initial condition to the whole model and as for the parts with 50 degrees we considered the temperature application in two different conditions. The first one considers the application of temperature only in the inner surface of the steel pipe and the second considers the whole boundary of the steel pipe to be at 50 degrees. This assumption is true due to two reasons, because the steel has relatively small thickness comparing to the whole geometry of the problem and the thermal conductivity of the steel is 25 times greater than that of concrete's, we know that the temperature of the steel will reach 50°C degrees very fast after the model has reached steady state conditions.

Stresses obtained from first set of conditions are presented in Figure 6. It is seen from it that the bigger stresses are registered in the elements in contact with water at 50°C temperature (left of the figure) and from this stresses to the right stresses are approximately ten times lower in the rest of the steel and the concrete pile.
Stresses registered using the second set of conditions are presented in Figure 7 show a more gradual variation of stresses in the pipe section and the concrete pile, keeping the stresses in the same range of results. This stress distribution is considered to be more accurate for the type of problem considered. Considering the temperature variation applied to the whole steel pipe is more realistic as we are evaluating a steady state problem without considering the effect of time. Because the stress distribution in the second case is much better than the first, we are assuming that water flows at a certain temperature for a period of time long enough to heat up the whole pipe section to the same temperature. This assumption is also used in the next cases.

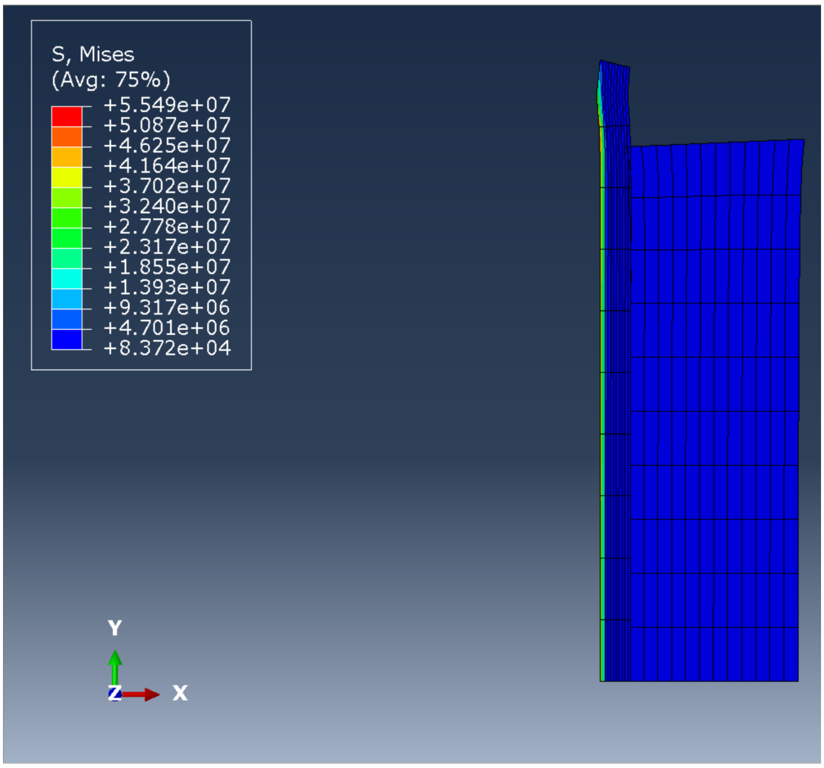

Figure 6: Von Misses stress distribution over the pile. Mechanical and thermal loads considered. Temperature in the inner surface of the pipe.

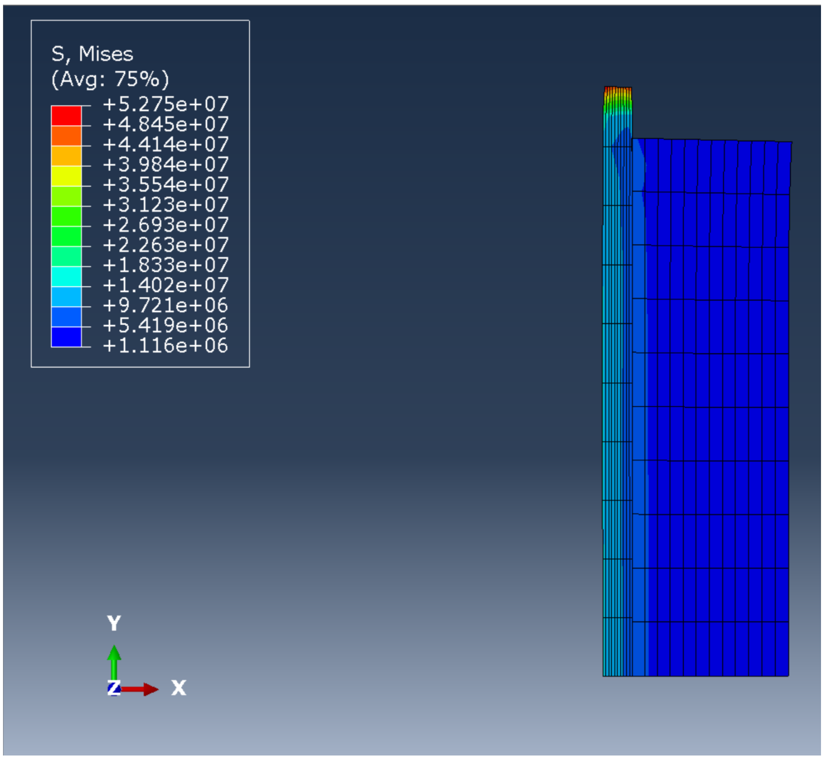

Figure 7: Von Misses stress distribution over the pile. Mechanical and thermal loads considered. Temperature applied to the whole steel width.

2.2.3 Maximum operating temperatures for steel and concrete considering plastic behaviour.

Analyze which is the maximum increase in water temperature that the steel pipe and the concrete can withstand if we consider that steel yields at 500 MPa and the concrete used has 30 MPa of characteristic cubic compressive strength. What would you change in the structure to increase the admissible water temperature?

In this point of the assignment the maximum water temperature is determined by increasing its temperature from 50°C using steps of ΔT = 10°C. At this part, it is important to define the maximum stresses the material will withstand. Therefore, the concrete characteristic cubic compressive strength is defined as $_{C}$=30 MPa, and the yield stress for the steel is defined as $_{S}$=500 MPa.
After four ΔT steps applied to the system, the concrete reached an stress of about σ_C=29.7 MPa. This value is near enough to the maximum stress that the concrete and the analysis is considered finished with a maximum water temperature of ninety degrees (T_{max} = 90 °C). Considering the stresses near yielding were registered in the concrete pile, the concrete cubic compressive strength can be easily increased to 35 MPa or 40 MPa.

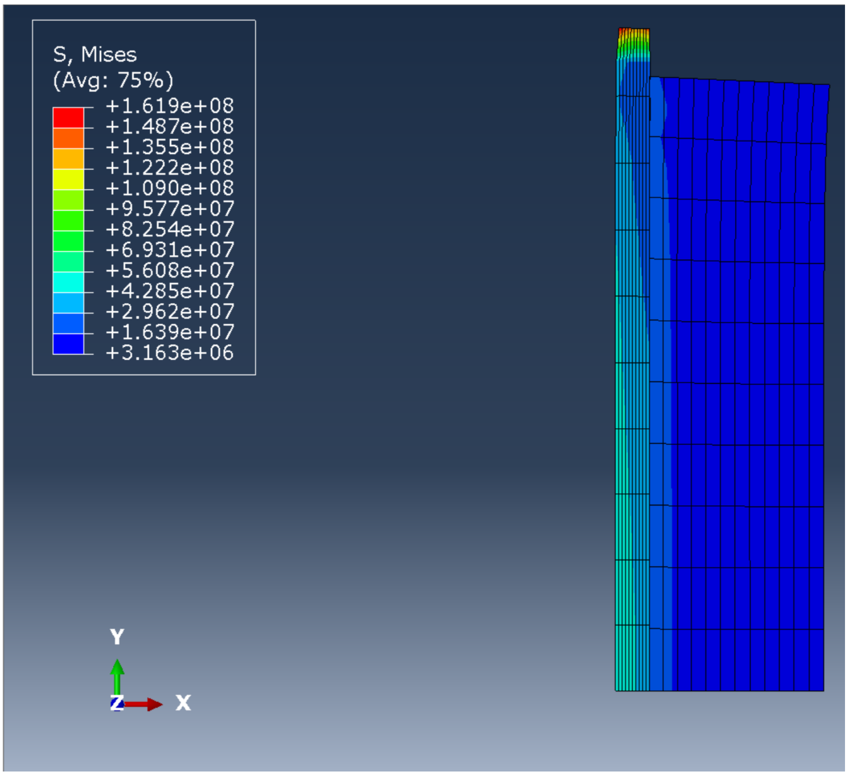

Figure 8: Von Misses stress distribution over the pile for an inner steel surface temperature of 90°C.

2.2.4 Evaluation of a temperature-dependent Young's Modulus

Assume we want to use a new type of concrete whose properties vary with temperature according to Table 2. How would this affect the results obtained in 2?

Temperature T [°C]	Young's modulus E [Pa]
15	$2.7 \cdot 10^{10}$
25	$3.5 \cdot 10^{10}$
35	$5.0 \cdot 10^{10}$
45	$7.0 \cdot 10^{10}$
55	$1.0 \cdot 10^{11}$

Table 2: Temperature dependent material properties of concrete.

Taking advantage of the material description capabilities of *ABAQUS*, Young's modulus was described for the temperatures given in Table 2 defining a scatter distribution and linear interpolation among the points. The obtained results can be found in Figure 9.
These results show that no important variation on the stresses are generated due to the temperature varying Young's modulus regarding to the maximum and minimum values registered. Even though the pile-pipe system does not register important variations on the stresses, it is pointed out that near the steel pipe, due to its deformations and the fact that this part of the system has the highest temperature (therefore the bigger Young's modulus), for differential deformations that the pipe transmits to the pile, bigger stresses are registered. In the concrete pile, but it is seen that a smoother transition of stresses is registered from the temperature dependent Young's modulus in comparison with the independent case. The reason that the answers do not vary significantly with the independent case is that because the step that we are using to simulate the model is static-general (3) so Abaqus does not calculate the temperature field at the boundaries and only considers the effect of the temperature as a thermo-stress in the model, therefore it uses the Young's modulus at 30°C and because in this case it is higher than the usual 27000 MPa the distribution of stress inside the concrete is more than the independent case.

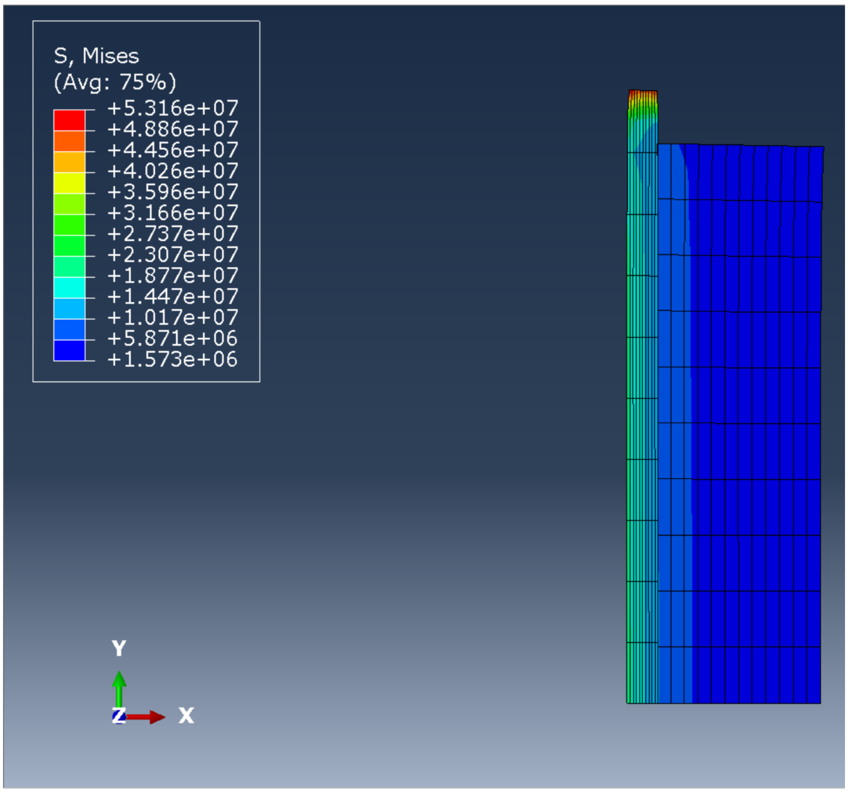

Figure 9: Von Misses stress distribution over a temperature-dependent concrete Young's Modulus.

3 Validation, verification and mesh convergence

3.1 Validation and verification

In order to verify if the model and specially the contact is working properly, we have done extra models of simple cases of the steel and the concrete separately in order to see if the stresses in each case are in the same scale as the general model. After modeling both the steel and the concrete and running the simulations we can see that the stresses in the concrete are in the range of 4.5 MPa and the stresses created in the steel are in the range of 7.5 MPa. The stresses are not the same as the general model because of the contact between the steel and the concrete in the general model but we can see that it is in the same scale, this verifies that the general model simulation.

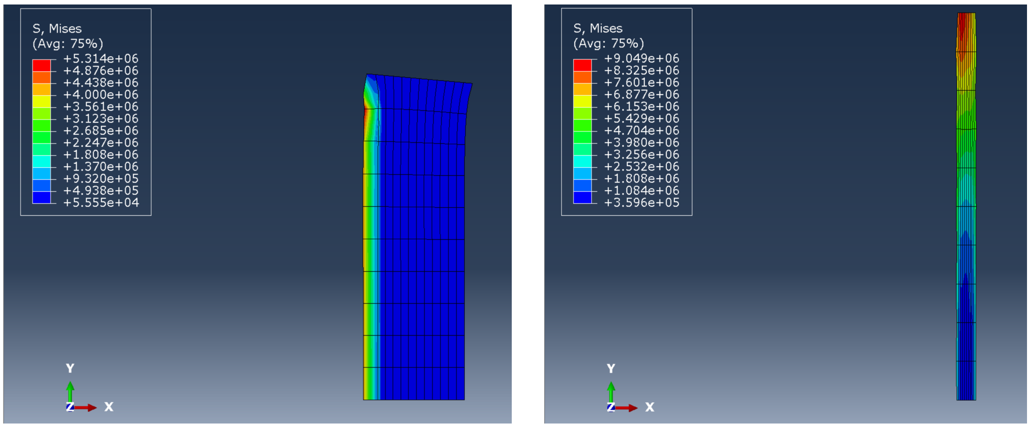

(a) Validation test of concrete (b) Validation test of the steel

Figure 10: Pile model.

3.2 Mesh convergence

In order to verify the answers provided by the model, a mesh convergence evaluation was performed. Linear and quadratic quadrilateral elements in a structured mesh were applied to the model. Since the model has two bodies in contact, the mesh convergence was carried out in both bodies. The chosen parameters for convergence test were the vertical displacements at specific nodes at the concrete part and the steel part. Figure 11 depicts the nodes (in colour red) at which the vertical displacements were analyzed. The mesh convergence evaluation was carried out in three parts. The first part aimed to verify how the element density (number of elements per unit area) in each body affects the convergence parameters. Such analysis considered only linear quadrilateral elements. Table111 presents the mesh features and the values for the vertical displacements in the concrete and the steel part for this step of the mesh convergence evaluation.

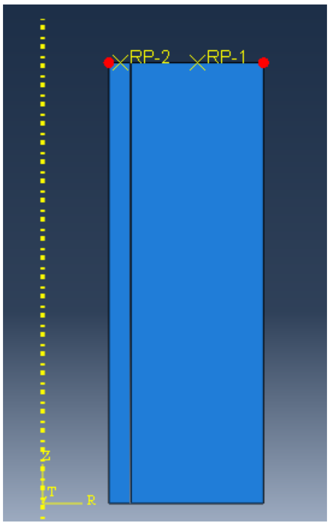

Figure 11: Nodes chosen for mesh convergence evaluation.

Elements in		Elements density in		Vertical displacement [mm]	
steel	concrete	steel	concrete	steel	concrete
10	60	200	200	0.122	-0.0078
20	60	400	200	0.063	-0.0098
20	120	400	400	0.063	-0.0098
30	120	600	400	0.042	-0.0092

Table 3: Element density influence of each body on convergence parameter.

According to Table 3, the number of elements in the steel body influences more the convergence parameters than the number of elements in the concrete body. The vertical displacements were more affected when the element density in the steel body increased , such as in meshes 3 and 4 in comparison with mesh 1. Considering this, the second part of mesh convergence evaluation verified .how the increase in the number of elements in a specific direction would affect the chosen convergence parameters. Such evaluation was also carried out using only linear quadrilateral elements.

Elements in width		Elements in height		Total elements	Vertical displacement [mm]	
steel	concrete	steel	concrete	steel/concrete	steel	concrete
3	30	10	10	30/300	0.042	-0.0092
5	30	10	10	50/300	0.025	-0.0083
5	30	20	20	100/600	0.026	-0.0081
6	30	20	20	120/600	0.021	-0.0078

Table 4: Influence on convergence parameters by number of elements in specific directions.

According to Table 4, the number of elements in the width direction affect the results more than the number of elements in the height direction. Taking into account the effect of each body's element density and the direction of discretization, new meshes were created to verify the convergence of the vertical displacements. For such evaluation, linear and quadratic quadrilateral elements were applied to the geometry. The CPU time of each simulation was also evaluated. Tables 5 and 6 present the meshes used for such study along with the CPU Time and Figures 12 and 13 present the convergence curves for the vertical displacements in the concrete and steel.

Elements in width		Number of elements			CPU
steel	concrete	steel	concrete	total	Time
1	6	10	60	70	0.6
2	6	20	60	80	0.7
2	12	20	120	140	1.0
3	12	30	120	150	0.8
3	30	30	300	330	1.0
5	30	50	300	350	1.0
5	30	100	600	700	1.5
6	30	120	600	720	1.4
10	30	200	600	800	1.3

Table 5: Meshes used for linear quadrilateral elements and CPU Time.

Elements in width		Number of elements			CPU
steel	concrete	steel	concrete	total	Time
1	3	10	30	40	0.8
1	6	10	60	70	0.9
2	6	20	60	80	1.0
3	6	30	60	90	0.8
3	12	30	120	150	0.9
5	12	50	120	170	1.1
6	12	60	120	180	1.0
10	12	100	120	220	1.0
10	15	100	150	250	1.0

Table 6: Meshes used for quadratic quadrilateral elements and CPU Time.

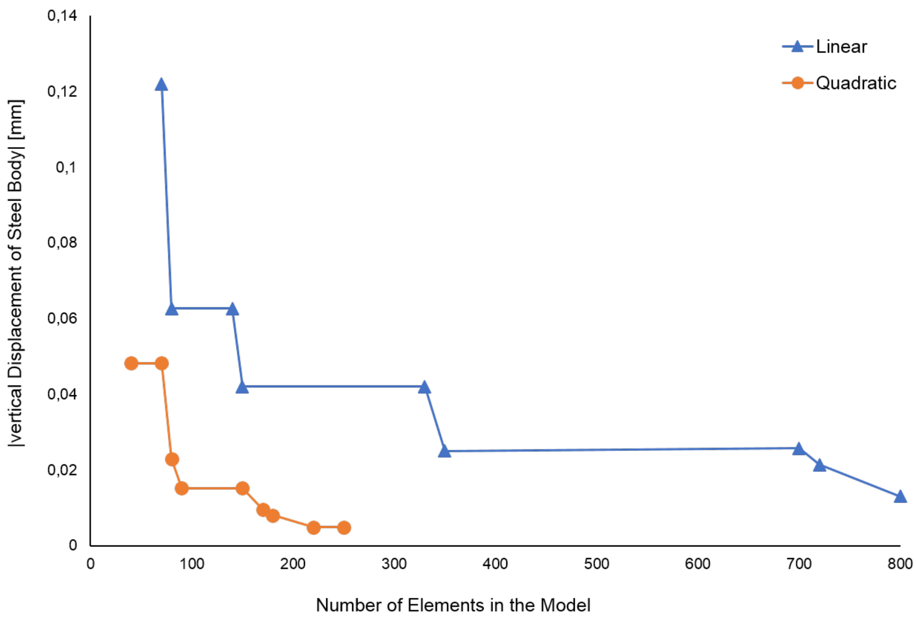

Figure 12: Convergence 1

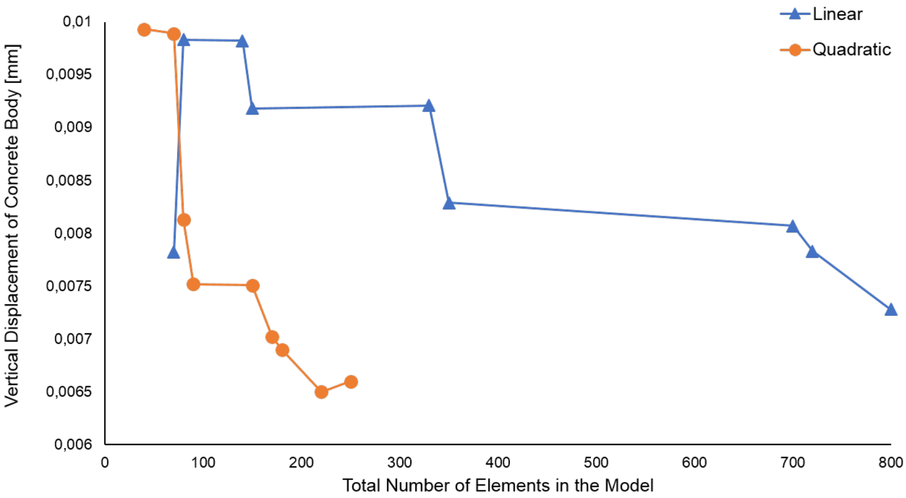

Figure 13: Convergence 2

Mesh 8 with quadratic quadrilateral elements was chosen as the most suitable among the tested meshes for the ongoing evaluations of the model. Mesh 8 provided appropriate results for the carried out analysis with fewer number of elements and reasonable CPU Time.

4 Conclusions

The subject chosen for the simulation project was *thermo-activated pile foundation* which is a clean and efficient way of obtaining energy from the soil using the foundation piles of a structure, by seizing the fact that the soil temperature at certain depth keeps constant throughout the whole year.
In addition to this gentle characteristic, soil structural capacity is used by installing a structural pile in the borehole made for obtaining energy. This document analyses the effects of thermal induced and structural loads by using a finite element method software for a slice of 1.0 m length at a representative depth of 20m.
The three-dimensional cylindrical problem was modelled as a axisymmetric two-dimensional problem, adapting the loads conditions and restraints necessary to fulfill the problem needs. Considering the different questions given on the assignment some conclusions are drawn:

- The effect of the structural load without any thermal effect does not generate significant stresses over the steel pipe and concrete pile;
- The coupled effect of considering thermal and structural loads generates bigger stresses;
- Applying the temperature variation to the total width of the steel pipe, given the relationship of steel width to pile width (0.1 times smaller), and steel thermal conductivity to pile thermal conductivity (25 times higher) generated a smoother transition of stresses through the system;
- The maximum water temperature, considering the yield stress for the two materials, was defined as 90°C, which is a high enough temperature for the water (ten degrees lower than its boiling temperature) and describes that the system is designed correctly. If an

improvement is required in the project, the concrete cubic compression strength can be higher up to 35 or 40 MPa;

- A temperature-dependent Young's modulus description was used and no significant changes were registered due to the non-transient calculation used for this model, as the design do not require this kind of analysis;
- Finally, a convergence analysis was executed using different element densities for the steel and the concrete, varying the amount of elements in horizontal and vertical directions and also using linear or quadratic element descriptions. The results shown that the convergence of the results was more influenced by the amount of elements in the horizontal direction, the density of elements in the steel pipe and that the quadratic element description was the most efficient selection.

Future works

As part of future works it would be interesting to analyse the effect of higher structural loads as for bigger buildings mainly analyzing the description of the soil thermal conductivity, the load capacity of the pile and characterize the expected settlements. It would be interesting to characterize the influence of thermal effects on the strength of the soil and analyse if this thermal branch may be the load determining the geometry of the pile.

Job division

- Renan Alessio: Convergence models and report chapter;
- Mariano Tomás Fernandez: Results interpretation, report and research;
- Aren Khaloian: Initial model set and resolution of assignment's tasks.

References

(1) Nicholson, D. P., Chen, Q., Pillai, A., Chendorain, M. (2013). Developments in thermal piles and thermal tunnel lining for city scale GSHP systems. Thirty-Eighth Workshop on Geothermal Reservoir Engineering, 1437–1444.

(2) Friction coefficient of steel on concrete or Grout, B.G. Rabbat, M.ASCE, H.G.Russell

(3) ABAQUS CAE Users's Manual.